NO Influence on Catalytic Soot Combustion: Lithium Nitrate and Gold Catalysts

María L. Ruiz,[†] Ileana D. Lick,[*,‡] María S. Leguizamón Aparicio,[‡] Marta I. Ponzi,[†] Enrique Rodriguez-Castellón,[§] and Esther N. Ponzi[‡]

[†]INTEQUI (CONICET-UNSL), 25 de Mayo No. 384, Villa Mercedes, San Luis, 5730, Argentina

[‡]Departamento de Química, Facultad de Ciencias Exactas, CINDECA (CCT-La Plata-CONICET-UNLP), calle 47 No. 257, La Plata, Buenos Aires, 1900, Argentina

[§]Departamento de Química Inorgánica, Crystalografía y Mineralogía, Facultad de Ciencias, Universidad de Málaga, Campus de Teatinos, Málaga, 29071, Spain

ABSTRACT: The diesel soot combustion was studied using catalysts prepared by impregnation with lithium nitrate and/or gold on zirconium oxide (ZrO_2), hydrated zirconium oxide, and silica (SiO_2). Catalysts were characterized by elemental analysis, atomic absorption spectrophotometry, X-ray diffraction (XRD), Fourier transform infrared spectroscopy (FTIR), transmission electron microscopy (TEM), and X-ray photoelectron spectroscopy (XPS). Measurements of catalytic activity were performed in a fixed bed reactor with a NO/O_2 feed. The NO reacts with the Li_2O generating "in situ" lithium nitrate that participates in the oxidation of diesel soot and accelerates the reaction rate. All catalysts containing lithium nitrate exhibit a good activity for soot oxidation, and the gold addition substantially increases selectivity to CO_2.

1. INTRODUCTION

A work published recently investigates the influence of nitrogen oxides on the soot combustion rate using cesium nitrate catalysts promoted with gold.[1] There is a fundamental difference between catalysts formulated with cesium nitrate and lithium nitrate. When the catalyst precursor containing cesium nitrate is calcined, the most abundant species is the cesium nitrate. In contrast, when the catalyst precursor containing lithium nitrate is calcined, part of lithium nitrate decomposes.[2]

The lithium nitrate decomposes thermally giving lithium oxide (Li_2O), nitrogen dioxide (NO_2), and oxygen (O_2).

$$4LiNO_3 = 2Li_2O + 4NO_2 + O_2 \qquad (1)$$
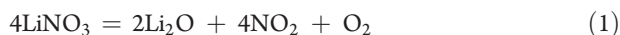
For lithium catalysts, the combustion in air occurs by catalysis with lithium oxide and the remaining nitrate is coordinated with the support.[3] The presence of nitrogen oxides in the feed can generate "in situ" nitrate ions. The catalyst with lithium nitrate generated "in situ" can be a catalyst more active than the catalyst containing lithium oxide.

The aim of this work is to study the influence of nitrogen oxides on the soot combustion rate using lithium nitrate catalysts and gold. Furthermore, several characterization techniques have been performed to study the nature of gold and lithium nitrate in these catalysts.

2. EXPERIMENTAL SECTION

2.1. Preparation of Catalysts. Three supports are used to prepare catalysts, silica (SiO_2), zirconium oxide crystallized in monoclinic phase (ZrO_2), and amorphous hydrated zirconium oxide ($ZrO_2 \cdot nH_2O$) prepared at the laboratory. Hydrated zirconium oxide ($ZrO_2 \cdot nH_2O$) was obtained by hydrolysis of zirconium oxychloride, $ZrOCl_2 \cdot 6H_2O$ (Fluka). The necessary

amount of aqueous ammonia (Tetrahedron 28%) was added to the zirconium oxychloride to reach a pH = 10. The product obtained by hydrolysis was filtered and washed until it was free from chloride ions, as determined by the silver nitrate test. The hydrated zirconium oxide ($ZrO_2 \cdot nH_2O$) thus obtained was dried at 80 °C for 24 h. This solid was then milled in a mortar and sieved to obtain particle sizes between 0.150 and 0.090 mm. The other supports, ZrO_2 and SiO_2, were commercial products provided by Anedra and Degussa, respectively.

Three series of catalysts were prepared with lithium nitrate and gold. Two of them have only a component (lithium nitrate or gold), and the third one has both components; the lithium nitrate is first impregnated and then the gold salt.

Catalysts containing gold were prepared by impregnation of supports. A gold solution was prepared from chloroauric acid trihydrate ($HAuCl_4 \cdot 3H_2O$) with 1% w/v concentration. This solution is added to the support, achieving the necessary volume to get a nominal gold concentration 2% w/w in the catalyst. With supports of $ZrO_2 \cdot nH_2O$ and ZrO_2, successive impregnations were made with intermediate drying. Meanwhile, for the SiO_2 support, the impregnation with Au was made with a more diluted solution to produce a better solid wetting.

For the preparation of catalysts with lithium nitrate, the impregnation of supports was carried out with an aqueous solution of lithium nitrate, in a rota-vapor equipment at 100 °C, rate of 170 rpm, and a vacuum pressure of 500 mmHg. The obtained solids were dried for 2 h at 80 °C and subsequently calcined at 600 °C for 1 h in air flow of 30 mL/min.

Catalysts containing lithium nitrate and gold were prepared by impregnation of supports with an aqueous solution of lithium nitrate as it was described above and, after the drying step, the impregnation with a solution of $HAuCl_4 \cdot 3H_2O$ was performed. The nomenclature has the lithium nitrate formula, and then, the gold symbol indicates the impregnation order, $LiNO_3AuSupport$.

Samples were prepared with a nominal concentration of 7.5% in weight of ion nitrate (8.34% in weight of lithium nitrate) and 2.0% in weight of Au. These precursors were dried at 80 °C for 24 h and subsequently calcined at 600 °C for 1 h in air flow of 30 mL/min.

In order to differentiate zirconia supports, the catalyst impregnated on ZrO_2 will be named Z and the catalyst prepared by impregnation of $ZrO_2 \cdot nH_2O$ will be named Zt. The silica will be named S. In this way, catalysts with lithium nitrate will be named $LiNO_3Z$, $LiNO_3Zt$, and $LiNO_3S$; gold catalysts will be named AuZ, AuZt, and AuS, and those ones with both species will be $LiNO_3AuZ$, $LiNO_3AuZt$, and $LiNO_3AuS$.

2.2. Characterization of Catalysts. Gold and lithium contents were determined by atomic absorption spectrophotometry with spectrophotometer Perkin-Elmer AA 3110. The elemental nitrogen content was determined by means of elemental analysis (EA) with a CHNS LECO 932 analyzer. Crystalline phases in the catalysts were identified by powder X-ray diffraction (XRD) analysis using a Rigaku D-Max III diffractometer equipped with Ni-filtered Cu Kα radiation ($\lambda = 1.5378$ Å).

The presence of nitrate anions on fresh and used catalysts was studied by means of Fourier transform infrared spectroscopy (FTIR) spectroscopy using an Spectrum RX1 Perkin-Elmer equipment. Spectra were recorded at room temperature in the $4000-400$ cm^{-1} range, and the samples were prepared in the form of discs with KBr.

The X-ray photoelectron spectroscopy (XPS) was performed with a Physical Electronics PHI-5700 spectrometer, equipped with a dual X-ray source of MgKα (1253.6 eV) and AlKα (1486.6 eV) and a multichannel detector. Spectra of powdered samples were recorded in the constant pass energy mode at 29.35 eV, using a 720 μm diameter analysis area. Charge referencing was measured against adventitious carbon (C1s at 284.8 eV). A PHI ACCESS ESCA-V6.0 F software package was used for acquisition and data analysis. A Shirley-type background was subtracted from the signals. Recorded spectra were always fitted using Gaussian–Lorentzian curves in order to determine the binding energy of the different element core levels more accurately.

Transmission electron microscopy (TEM) micrographs were obtained using a Phillips CM 200 Supertwin-DX4 microscope. Samples were dispersed in ethanol; a drop of the suspension was put on a Cu grid (300 mesh). Oxidation experiments of nitrite ion with or without catalysts were carried out in a thermobalance Shimadzu TA-50 with a feed air/He (40/20) and heating rate 10 °C/min.

2.3. Measurements of Catalytic Activity. Catalytic tests using O_2/inert feed or O_2/NO/inert feed were performed in a temperature programmed oxidation (TPO) apparatus, a fixed bed quartz microreactor with analysis of reaction gases. The microreactor was heated electrically. The reaction mixture was obtained from three feed lines individually controlled: NO/He, O_2/He, and He to close the balance. To study the soot combustion reaction, the reactor was fed with the following mixture: 1500 ppm of NO and 8% of O_2 (Q total = 50 mL/min).

Table 1. Concentration of Lithium, Gold, and Nitrate Ion

	% Li	% Au	% NO$_3^-$
LiNO$_3$S	0.74		0.74
LiNO$_3$Z	0.8		0.8
LiNO$_3$Zt	0.45		0.6
AuS		1.5	
AuZ		1.6	
AuZt		2.0	
LiNO$_3$AuS	0.72	2.0	0.2
LiNO$_3$AuZ	0.73	2.0	0.1
LiNO$_3$AuZt	0.74	2.0	0.1

The microreactor was loaded with 30 mg of catalyst and 3 mg of soot (Printex−U), and the combustion was carried out in the range of 200−600 °C with a heating rate of 2 °C/min. Before the reaction, the soot was mixed with the catalyst, with a spatula (loose contact). Reaction products were monitored with a gas chromatograph, Shimadzu model GC-8A, provided with a TCD detector. The sampling was carried out approximately every 8 min. The separation of products was performed with a concentric column CTRI of Alltech. This system permitted the identification and quantification of the peaks of O_2, N_2, CO_2, and CO. The concentration of CO_2 and CO was determined from the area of CO_2 and CO peaks obtained by chromatographic analysis.

3. RESULTS AND DISCUSSION

3.1. Characterization Results. *3.1.1. Chemical Analysis.* Catalysts were formulated with the following nominal concentrations: 2.0% (w/w) gold, 0.84% (w/w) lithium, and 7.5% (w/w) nitrate ion. Table 1 shows results of the concentration of gold and lithium (AAS) and nitrogen (EA) expressed as NO_3^-.

In catalysts that contain lithium, $LiNO_3$/support, and $AuLiNO_3$/support, the lithium content (AAS) is similar to the nominal one. Instead, the ion nitrate concentration, estimated from the elemental nitrogen concentration, is markedly lower than the nominal (7.5%), which indicates that an important part of supported lithium nitrate has decomposed in oxides (Li_2O) during precursor calcinations. The addition of chloroauric acid ($HAuCl_4$) in the preparation stage of catalysts generates a decrease of the supported nitrate concentration; this result is similar to the one found with cesium nitrate−gold supported catalysts.[1] The lithium nitrate has been transformed in other species during calcination of precursors that contain $HAuCl_4$.

The decomposition of $HAuCl_4 \cdot 3H_2O$ takes place as follows[4,5]

$$HAuCl_4 \cdot 3H_2O = HCl + AuCl_3 + 3H_2O \qquad (2)$$

$$AuCl_3 = Cl_2 + AuCl \qquad (3)$$

$$2AuCl = 2Au + Cl_2 \qquad (4)$$

Reactions represented in eqs 2 and 3 are possible between 120 and 175 °C, while the decomposition of AuCl to Au^0 and molecular chlorine (eq 4) is thermodynamically feasible from 250 °C.

The chlorine (Cl_2) generated during the calcination stage of samples (eq 4) in the catalyst preparation, can react with part of

Table 2. Gibbs Free Energy Change for Reactions 4 and 5

temperature (°C)	$\Delta G°$ eq 4 (kJ)	$\Delta G°$ eq 5 (kJ)
100	18.4	78.2
150	11.4	59.8
200	4.5	41.5
250	−2.3	23.5
300	−8.9	10.3
350	−15.5	−2.2
400	−21.9	−14.2
450	−28.2	−26.0
500	−34.4	−37.5

lithium nitrate according to eq 5.

$$Cl_2(g) + 2LiNO_3 = 2LiCl + O_2(g) + 2NO_2(g) \quad (5)$$
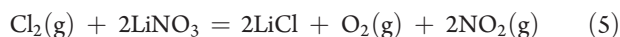
This reaction is thermodynamically feasible from 350 °C. These conclusions are based on the thermodynamic calculations presented in Table 2. For this reason, a chemical reaction between chlorine and lithium nitrate, catalysts that contain gold, has lower nitrate content than the LiNO$_3$/support catalysts. The gold concentration in AuZ and AuS catalysts is slightly lower than the nominal (2.0%) while it is similar to the nominal in catalysts containing lithium nitrate and gold.

3.1.2. X-ray Diffraction. Figure 1A–C shows XRD diagrams of all catalysts containing gold. Figure 1A shows diffraction diagrams of catalysts supported on silica, AuS, and LiNO$_3$AuS, and signals corresponding to metallic gold are observed (2θ: 38.18°, 44.39°, and 64.58°). These results are the ones expected from decomposition reactions of chloroauric acid trihydrate, HAuCl$_4$·3H$_2$O, presented in eqs 2, 3, and eq 4.

The diffraction line of metallic gold in AuZ and LiNO$_3$AuZ catalysts (Figure 1B) is not so marked as in catalysts supported on SiO$_2$; here, it is possible to observe only the diffraction line with highest intensity at 2θ: 38.18. The zirconia used as support is a commercial zirconia with monoclinic structure (($2\theta = 28.2°$, 31.5°, and 34.5°).
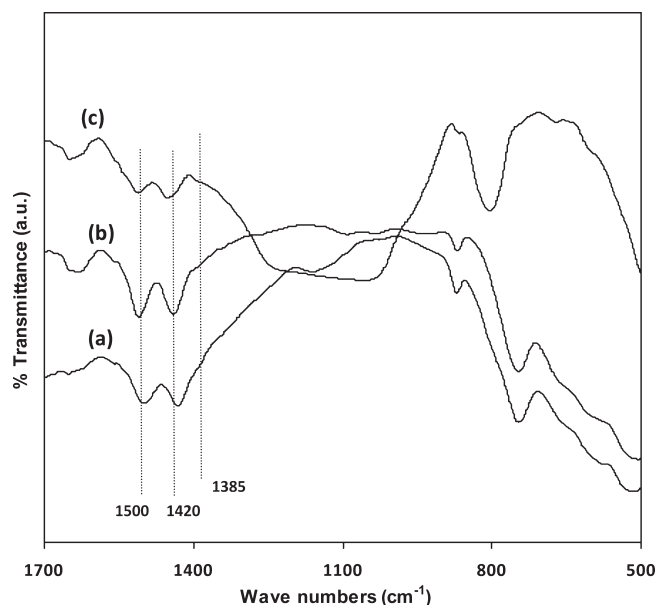
Figure 1C shows metallic gold signals in catalysts prepared from hydrated zirconia oxide, AuZt, and LiNO$_3$AuZt. The ZrO$_2$·nH$_2$O used as support is amorphous and adopts its crystalline structure after being impregnated and calcined showing diffraction lines corresponding to monoclinic and metastable tetragonal phases ($2\theta = 30.5°$, 35.2°, and 50.7°). The undoped and amorphous support adopts the monoclinic structure when it is calcined. The LiNO$_3$AuZt catalyst presents metastable tetragonal structure indicating a strong ion–support interaction generated in the crystallization stage. The presence of alkaline ions, in this case lithium, promotes the formation of the metastable tetragonal crystalline phase as it has been reported in previous works.[6,7] This interaction metal–support can be originated with the lithium incorporation to the network and the consequent generation of oxygen vacancies. On the other hand, the AuZt catalyst preferably presents monoclinic structure. No diffraction lines of lithium crystalline compounds are observed (Li$_2$O, Li$_2$O$_2$, LiNO$_3$, LiNO$_2$) in diagrams of catalysts presented in this work.

3.1.3. Infrared Spectroscopy (FTIR). Analyses by FTIR were performed in order to study the presence of nitrogen oxo species (nitrate ions, nitrite ions) in catalysts. Figure 2 shows FTIR spectrum of catalysts containing lithium nitrate and gold, LiNO$_3$AuZ, LiNO$_3$AuZt, and LiNO$_3$AuS catalysts. Spectra show
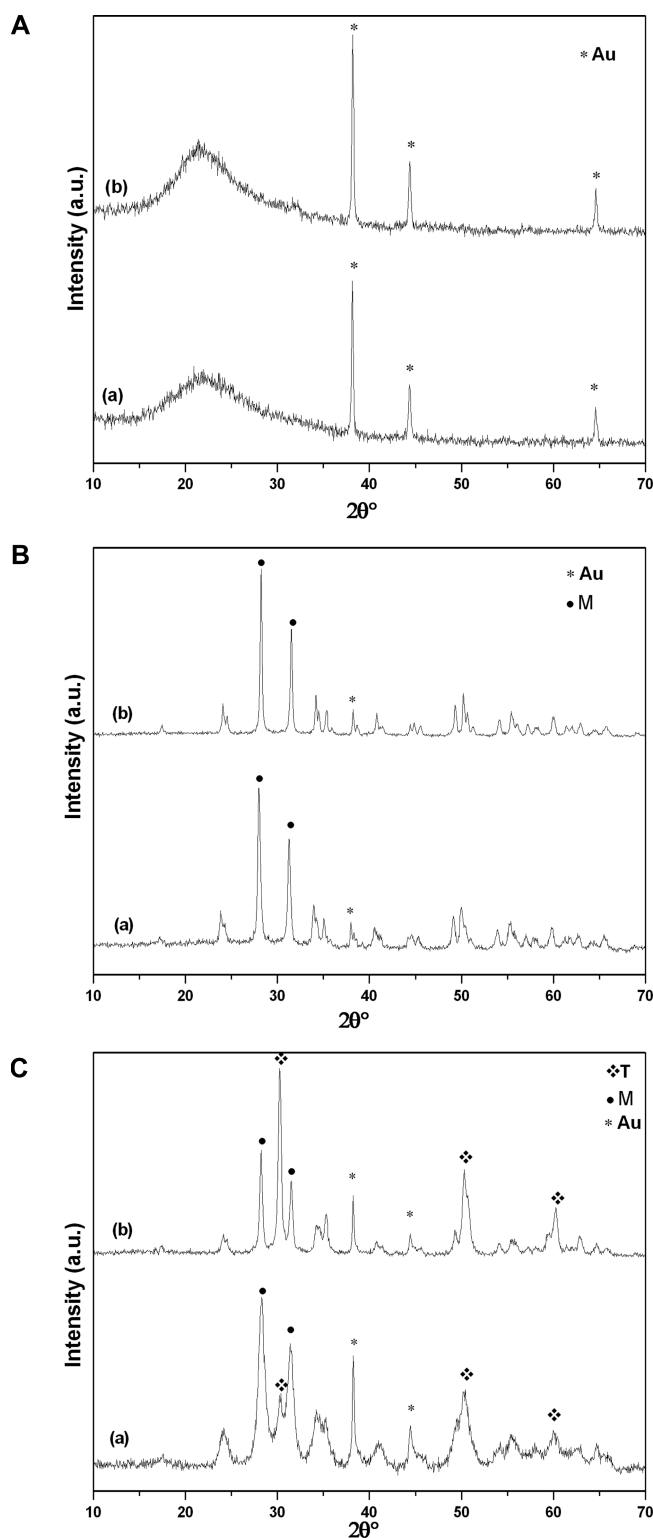
Figure 1. X-ray diffraction diagrams. (A) Catalysts supported on silica. (a) AuS; (b) LiNO$_3$AuS. (B) Catalysts supported on commercial zirconia. (a) AuZ; (b) LiNO$_3$AuZ. (C) Catalysts prepared from amorphous zirconia. (a) AuZt; (b) LiNO$_3$AuZt.

signals associated with the presence of nitrate ions coordinated with the support,[8] which are presented at 1420 and 1500 cm^{-1}. Neither the typical signal of free nitrate ions (1385 cm^{-1}) nor the signal of free nitrite ions (1360 cm^{-1}) are observed in spectra.
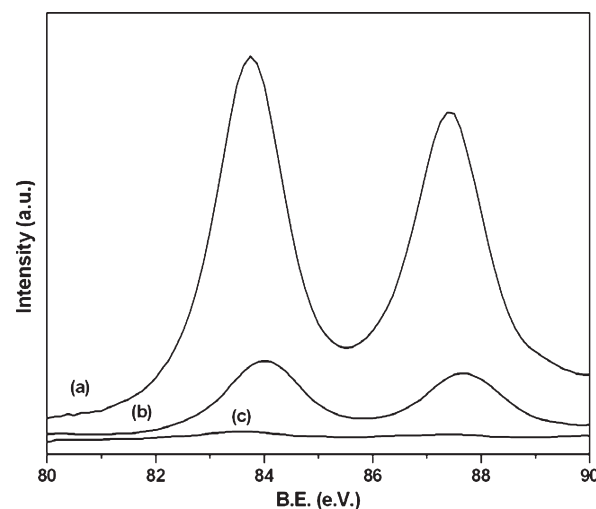
Figure 2. FTIR spectra of catalysts. (a) $LiNO_3AuZt$; (b) $LiNO_3AuZ$; (c) $LiNO_3AuS$.

Figure 3. X-ray photoelectron spectroscopy for the region of Au $4f_{7/2}$. (a) $LiNO_3AuZt$; (b) $LiNO_3AuZ$; (c) $LiNO_3AuS$.

Table 3. XPS Results for Catalysts (all BE values in eV)

sample	O 1s		Si 2p	Zr 3d		Au 4f$_{7/2}$		Li 1s
S	532.9		103.7					
Z	532.0	530.2		184.7	182.3			
Zt	531.5	529.7		184.3	181.9			
AuSi	533.0		103.0			86.8	83.5	
AuLiS	532.6		103.4			86.8	83.3	55.3
AuZ	532.9	530.6		185.0	182.6	87.6	84.0	
AuLiZ	532.0	530.1		184.6	182.2	87.7	84.1	55.3
AuZt	532.6	530.4		184.8	182.4	87.3	83.7	
AuLiZt	532.3	530.3		184.5	182.1	87.2	83.6	55.3
Li Si	532.7		103.4					54.9
Li Z	530.0	530.4		184.5	182.1			55.3
LiZt	532.0	529.9		184.3	181.9			55.3

Catalysts containing only lithium nitrate, $LiNO_3Z$, $LiNO_3Zt$, and $LiNO_3S$, present weak energy absorption bands associated to the presence of free nitrate ions and nitrates coordinated with the support.[3]

3.1.4. Photoelectron Spectroscopy (XPS). XPS spectra of gold catalysts AuZ, AuZt, and AuS and lithium nitrate and gold catalysts, $LiNO_3AuZ$, $LiNO_3AuZt$, and $LiNO_3AuS$ were performed. The position of gold, lithium, oxygen, and zirconium emission bands was determined from spectra, and results are shown in Table 3. Figure 3 shows XPS spectra for the Au $4f_{7/2}$ region of the $LiNO_3AuZ$, $LiNO_3AuZt$, and $LiNO_3AuS$ catalysts. The Au $4f_{7/2}$ signal is observed in all catalysts centered at 83.9 eV. This signal is assigned to metallic Au. Photoemissions at 85.7 eV and 87.1 eV are not observed. These are the value found in the literature for Au_2O_3.[9] Neither photoemissions are observed at 86.3 eV, attributed to the presence of ionic gold species. Results obtained by XPS are in agreement with those obtained by XRD which show diffraction lines of metallic gold and reject the

possibility that a small portion of superficial gold is found as oxidic phases.

On the other hand, it is possible to observe that the binding energies (BE) of gold are not affected by the lithium presence. In this same sense, the BE of lithium are not affected by the gold presence.

The bulk atomic ratio Li/Z in catalysts is 0.125 when calculated from AAS measurements. The surface atomic ratio determined by XPS is higher than that observed for the bulk in catalysts $LiNO_3$/support and $LiNO_3Au$/support, which indicates that most lithium remains on the surface, fundamentally, in catalysts $LiNO_3Z$ and $LiNO_3AuZ$ that were prepared with monoclinic zirconia of low surface area and pre-established crystalline structure.

The Li/Zr atomic ratio is lower in catalysts prepared from hydrated zirconium oxide $(ZrO_2 \cdot nH_2O)$ than the Li/Zr ratio obtained for catalysts prepared from monoclinic zirconia. This is due to the fact that part of lithium is incorporated to the structural zirconia network that originally is an amorphous solid and with large surface area $(400 \ m^2/g)$. The incorporation of lithium is further supported with a change of crystalline structure as it has been shown by XRD.

The surface Li/Zr atomic ratio is lower for $LiNO_3AuZ$ catalyst than that observed for $LiNO_3Z$ catalyst, which suggests that part of lithium atoms are found covered by gold clusters. The catalyst $LiNO_3AuZ$ presents a higher surface Au/Zr atomic ratio than that observed for AuZ catalyst, even when the gold concentration is the same in both catalysts. These results suggest that the presence of lithium nitrate generates more dispersed gold species on this support.

Analyses of the superficial atomic concentrations were carried out. Table 4 shows the surface atomic concentration ratios Li/Zr, Li/Si, Au/Zr, and Au/Si for the series of catalysts Au/support, $LiNO_3$/support, and $LiNO_3Au$/support. The bulk atomic ratio Li/Zr in catalysts is 0.125 when calculated from AAS measurements. The surface atomic ratio determined by XPS is higher than that observed for the bulk in catalysts $LiNO_3$/support and $LiNO_3Au$/support, which indicates that most lithium remains on the surface, fundamentally, in catalysts $LiNO_3Z$ and $LiNO3AuZ$

that were prepared with monoclinic zirconia of low surface area and pre-established crystalline structure.

The Li/Zr atomic ratio is lower in catalysts prepared from hydrated zirconium oxide $(ZrO_2 \cdot nH_2O)$ than the Li/Zr ratio obtained for catalysts prepared from monoclinic zirconia. This is due to the fact that part of lithium is incorporated to the structural zirconia network that originally is an amorphous solid and with large surface area $(400 \ m^2/g)$. The incorporation of lithium is further supported with a change of crystalline structure as it has been shown by XRD.

The surface Li/Zr atomic ratio is lower for $LiNO_3AuZ$ catalyst than that observed for $LiNO_3Z$ catalyst, which suggests that part of lithium atoms are found covered by gold clusters. The catalyst $LiNO_3AuZ$ presents a higher surface Au/Zr atomic ratio than that observed for AuZ catalyst, even when the gold concentration is the same in both catalysts. These results suggest that the presence of lithium nitrate generates more dispersed gold species on this support.

3.1.5. Transmission Electron Microscopy (TEM). Figure 4A,B shows micrographs of AuZt and $LiNO_3AuZt$ catalysts; the reference scale is 200 nm for both cases, and Table 5 presents the range of gold crystal sizes of all catalysts. It is evident that the lithium nitrate presence provides smaller gold crystals when the support is tetragonal zirconia (Zt). These results are in agreement with that observed by XPS, showing a higher atomic ratio (Au/Zr) when the catalyst was formulated with lithium nitrate.

In AuZ and AuZt catalysts, the lithium nitrate addition generates a decrease in the size of gold crystals; instead, the effect is opposite on silica, the lithium nitrate addition generates a minor dispersion of gold particles. This higher dispersion could be generated during the impregnation stage of the catalysts. It is known that the zirconia may have surface vacancies and that electrons can be trapped into these vacancies. When impregnating the support with the acid $HAuCl_4$, the gold is
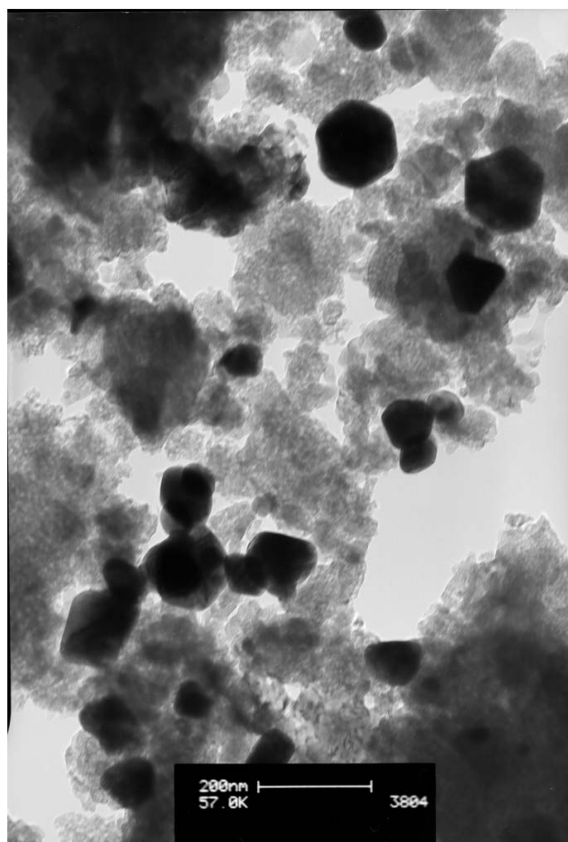
Table 4. Superficial Atomic Ratio Li/Zr, Li/Si, Au/Zr, and Au/Si

	Li/Zr	Li/Si	Au/Zr	Au/Si
AuZ			0.021	
AuZt			0.052	
AuS				0.0004
$LiNO_3AuZ$	5.21		0.036	
$LiNO_3AuZt$	2.64		0.055	
$LiNO_3AuS$		0.010		0.0010
$LiNO_3Z$	10.21			
$LiNO_3Zt$	2.99			
$LiNO_3S$		0.140		

Table 5. Gold Crystal Size

catalyst	crystal sizes (nm)
AuZ	100−800
$LiNO_3AuZ$	65−650
AuZt	65−125
$LiNO_3AuZt$	30−60
AuS	210−580
$LiNO_3AuS$	285−800
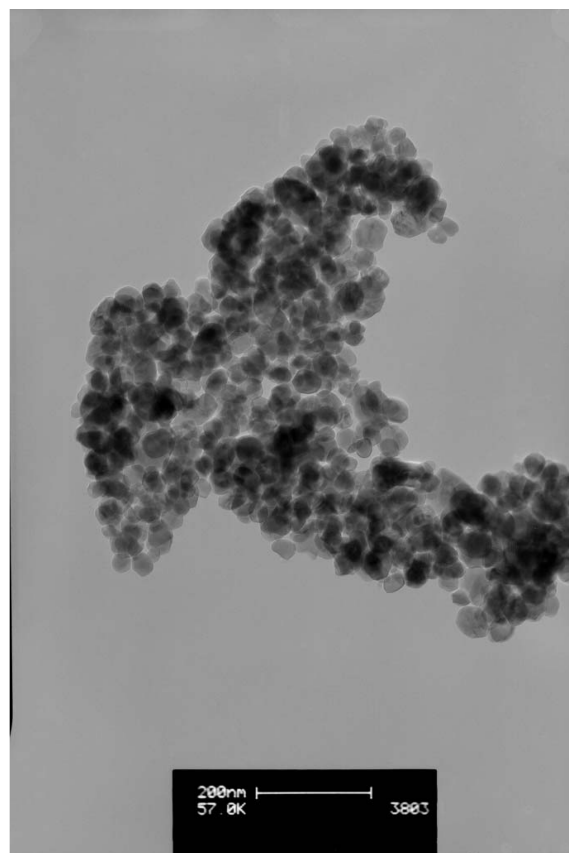
Figure 4. (A) TEM micrograph of AuZt catalyst. (B)

1154

dx.doi.org/10.1021/ie201295s |*Ind. Eng. Chem. Res.* 2012, 51, 1150–1157

A

B
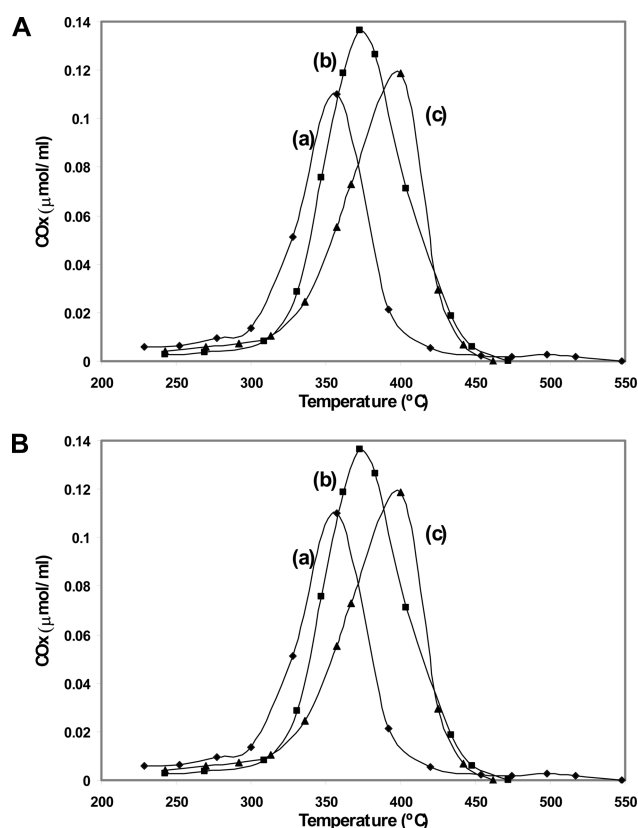
Figure 5. (A) Soot combustion, feed with NO. (a) $LiNO_3AuZ$; (b) $LiNO_3AuZt$; (c) $LiNO_3AuS$. (B) Soot combustion, feed without NO. (a) $LiNO_3AuZ$; (b) $LiNO_3AuZt$; (c) $LiNO_3AuS$.

found as $[AuCl_4]^-$ anions, with coplanar square structure. These anions can be deposited in the oxygen vacancies[10] near the sites Zr^{4+}/Zr^{3+}. In catalysts containing lithium, part of this lithium can remain on the surface as Li_2O where lithium is providing its electropositive character. Other parts as lithium nitrate and the remainder may be part of the structural network with the consequent oxygen vacancies and therefore higher possibility of deposition sites of the anion. Then, the process is completed during calcination at a high temperature, and a possible agglomeration of gold atoms to give Au^0 clusters of big size occurs.[10,11] The formation of these clusters is more evident in the case of silica, which has neither possibility of generating strong interactions with the lithium nor with the gold while loosing its superficial hydroxyl groups during the calcination treatment. The addition of alkaline metals also generates gold particle size decrease in catalysts supported on TiO_2.[12]

3.2. Catalytic Results. *3.2.1. Catalytic Results Obtained in a Fixed Bed Reactor Fed with NO/O₂.* Catalytic measurements for the soot oxidation were performed in a fixed bed reactor fed with oxygen and nitrogen oxides, and the soot catalyst mixture is made with spatula ("loose contact"). Figure 5A,B shows catalytic results obtained in a fixed bed reactor with $LiNO_3AuS$, $LiNO_3AuZ$, and $LiNO_3AuZt$ catalysts using a $NO/O_2/He$ and O_2/He mixture. Curves represent the combustion evolution of soot as function of the temperature.

Figure 5A shows the activity of $LiNO_3Au$/support catalysts when the reactor is fed with a $NO/O_2/He$ mixture. The $LiNO_3AuZ$ catalyst, the most active of the series, is the

Table 6. Temperature of Maximum Combustion Rate[a]

	T_{max} (°C)		
catalyst	$O_2/NO/He$	O_2/He	ΔT (°C)
without catalyst	580	590	10
AuZ	549	587	39
AuZt	526	590	64
AuS	567	590	23
$LiNO_3Z$	367	448	81
$LiNO_3Zt$	355	451	96
$LiNO_3S$	467	512	45
$LiNO_3AuZ$	357	395	54
$LiNO_3AuZt$	373	410	37
$LiNO_3AuS$	400	522	122

[a] Reaction with and without NO. $LiNO_3$/support and $LiNO_3$/Au/support catalysts.

Table 7. Gibbs Free Energy Change for Reactions of Carbon Oxidation, Carbon Monoxide, and Lithium Nitrite

| T (°C)	$\Delta G°$ eq 6 (KJ)	$\Delta G°$ eq 7 (KJ)	$\Delta G°$ eq 8 (KJ)
100	−61.8	−500.7	−164.3
200	−79.4	−483.2	−146.3
300	−96.5	−465.6	−130.8
400	−110.4	−448.1	−120.8

catalyst that presents the highest surface atomic ratio of lithium (Li/Zr = 5.21).

Figure 5B shows the activity of $LiNO_3Au$/support catalysts when the reactor is fed with an O_2/He mixture without NO. Activity showed the same trend as in the previous case

Table 6 shows the NO influence on the temperature corresponding to the maximum combustion rate. In this table, results obtained with Au/support and $LiNO_3$/support catalysts are included.[1,3]

Catalysts containing lithium nitrate are much more active than catalysts containing only gold; for this reason, it is supposed that the reaction starts with the oxidation of soot carbon with the lithium nitrate giving lithium nitrite, and then it reoxidizes with the oxygen of the feed flow or from the support.

$$C + LiNO_3 = CO + LiNO_2 \qquad (6)$$

$$CO + \frac{1}{2}O_2 = CO_2 \qquad (7)$$

$$LiNO_2 + \frac{1}{2}O_2 = LiNO_3 \qquad (8)$$
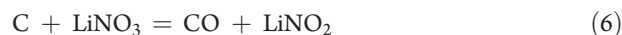
The three previous reactions are spontaneous within the temperature range in which the catalytic soot combustion occurs. Table 7 shows values of free energy for each one of the reactions.

The gold addition increases the soot combustion rate when the feed is air and the support is zirconia, but the same does not occur with the catalyst supported on silica. The gold addition results in a decrease of nitrate ion concentration in all catalysts from 0.6 to 0.8% to 0.1−0.2%. The decrease of nitrate ion concentration can lead to an activity decrease. On the other hand, the gold is a noble metal that presents catalytic properties for oxidation when it is found in small crystals. Schubert et al.[13]

1155

dx.doi.org/10.1021/ie201295s |*Ind. Eng. Chem. Res.* 2012, 51, 1150–1157

A

B
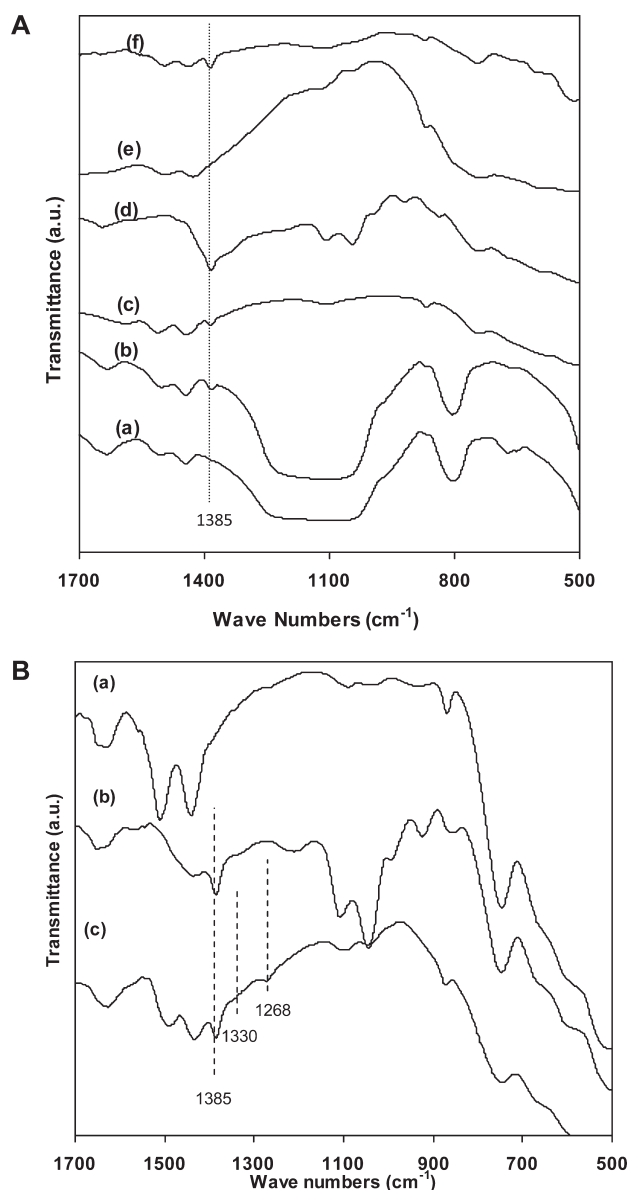
Figure 6. (A) FTIR spectra of catalysts used in presence of NO/O_2. (a) $LiNO_3S$ fresh; (b) $LiNO_3S$ used; (c) $LiNO_3Zt$ fresh; (d) $LiNO_3Zt$ used; (e) $LiNO_3Z$ fresh; (f) $LiNO_3Z$ used. (B) FTIR spectra of catalysts (a) $LiNO_3AuZt$ fresh, (b) $LiNO_3AuZt$ used in NO/O_2, and (c) $LiNO_3AuZt$ used in the soot combustion in an inert atmosphere.

studied the influence of the support on the gold activity and the possible reaction mechanisms. They found that catalysts that use inert materials as supports such as SiO_2 are less active for oxidation and can show good activity if only a high dispersion value of gold particles exists. In the catalyst supported on silica ($LiNO_3AuS$), no small gold crystals exist and it is the catalyst that does not increment the activity compared with the catalyst without gold ($LiNO_3S$). Results of Table 6 show that the NO addition in the feed increases the combustion rate in all catalysts, in those containing only one component (Au o $LiNO_3$) as well as in the ones that contain both components (Au and $LiNO_3$).

In catalysts with lithium compounds, the NO can react with the lithium oxide and form "in situ" the lithium nitrite that then it oxidizes with the oxygen of the air or of the support (zirconia)
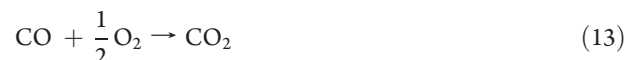
to lithium nitrate.

$$Li_2O + 2NO + \frac{1}{2}O_2 \leftrightarrow 2LiNO_2 \tag{9}$$

$$LiNO_2 + \frac{1}{2}O_2 \leftrightarrow LiNO_3 \tag{10}$$

Another alternative is to suppose that the NO of the gaseous phase in air oxidizes to NO_2 and that the NO_2 reacts with the lithium oxide to generate "in situ" lithium nitrate with its wetting properties and redox properties:

$$2NO + O_2 \leftrightarrow 2NO_2 \tag{11}$$

$$2NO_2 + Li_2O + \frac{1}{2}O_2 \leftrightarrow 2LiNO_3 \tag{12}$$
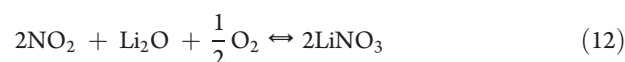
Catalysts promoted with gold can accelerate the transformation reaction of NO to NO_2 and in this way to increase the formation rate of lithium nitrate "in situ".[1] The "in situ" nitrate formation can be demonstrated in lithium catalysts and gold–lithium catalysts. Figure 6A shows FTIR spectra of fresh and used $LiNO_3$/support catalysts. The used catalysts are samples extracted from the reactor after being used in the reaction. In spectra of used samples in presence of NO/O_2, the intensity of the antisymmetric stretching band of free nitrate species located at 1385 cm^{-1} increased compared with the fresh catalyst.

In all spectra of used $AuLiNO_3$ catalyst, the antisymmetric stretching band of free nitrate species (1385 cm^{-1}) appears. These bands are not observed in the fresh catalysts (Figure 2). This effect is more evident in the $AuLiNO_3Zt$ catalyst (Figure 6B). In this same figure, the spectrum of a sample of this catalyst extracted from a fixed bed reactor after a reaction between soot and active phases of catalysts in an inert helium atmosphere at 360 °C is shown. In this FTIR spectrum, it is possible to observe an energy absorption band at 1330 cm^{-1} assigned to symmetric N–O stretching and another at 1268 cm^{-1} assigned to antisymmetric N–O stretching of free nitrite species.[14]

These results suggest that NO increases activity by generation of the "free nitrate" species over the Li_2O.[3] Another reaction accelerated by the higher oxygen transfer generated by gold is the oxidation of carbon monoxide generated in the first step giving CO_2:

$$CO + \frac{1}{2}O_2 \rightarrow CO_2 \tag{13}$$

Catalysts containing only lithium nitrate are active, but they give as secondary product CO (2% of CO_x). The addition of gold substantially increases the CO_2 generation, leading to a 100% of selectivity to CO_2.

3.2.2. Catalytic Oxidation of Nitrite Ion (NO_2^-) in Air. In this paper, it is proposed that one step of the catalytic cycle is the nitrite ion oxidation to nitrate ion. Catalytic oxidation experiments are carried out in a thermobalance using a sample of 10 mg of potassium nitrite salt and a gaseous feed of air and helium (air/He 2:1). The potassium nitrite salt and the catalyst (KNO_2/catalyst: 1/1) are milled in a mortar to obtain tight contact.

Figure 7 shows nitrite ion oxidation results with air using all catalysts supported on monoclinic zirconia. The nitrite ion oxidation starts approximately at 580 °C without catalyst, and when the support or catalysts are used, the oxidation begins at much lower temperature between 300 and 400 °C. Results show
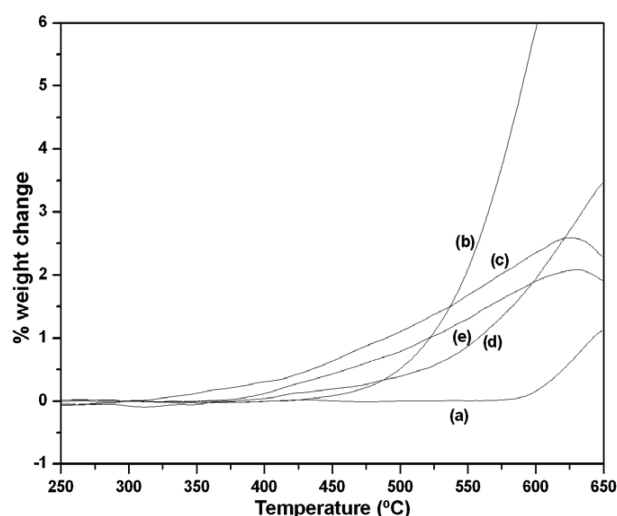
Figure 7. Potassium nitrite oxidation in air flow. (a) Without catalyst; (b) ZrO_2; (c) $LiNO_3Z$; (d) AuZ; (e) $LiNO_3AuZ$.

that nitrite is oxidized more rapidly with oxygen transferred by the support than the oxidation by oxygen in the gas phase.

4. CONCLUSIONS

The catalysts with lithium nitrate and gold are more active than catalysts containing only gold. This behavior is attributed to the wetting capacity of the catalytic surface given by the $LiNO_3$ and of low melting point, as well as to nitrate species involved in the redox cycle, eqs 2–4.

The gold addition increases the soot combustion rate when the feed is air and the support is zirconia, but the same does not occur with the catalyst supported on silica. $LiNO_3Au$/zirconia catalysts have small gold crystals (30 to 65 nm) while $LiNO_3$/silice catalysts have larger crystals (285 nm), and it is supposed that they do not promote the oxidation.

The NO addition in the feed accelerates the combustion rate in all catalysts in those that contain only one component (Au or $LiNO_3$) as well as in those ones that contain both components (Au and $LiNO_3$). The LiAuZ catalyst is the most active and presents higher lithium surface concentration. The gold addition substantially increases the CO_2 generation leading to 100% of selectivity to CO_2.

■ AUTHOR INFORMATION

Corresponding Author
*E-mail: ilick@quimica.unlp.edu.ar.

■ ACKNOWLEDGMENT

■ REFERENCES

(1) Ruiz, M. L.; Lick, I. D.; Ponzi, M. I.; Rodriguez-Castellón, E.; Jiménez-López, A.; Ponzi, E. N. Combustion of diesel soot in NO/O_2 presence. Cesium nitrate and gold catalysts. *Appl. Catal., A* **2011**, *392*, 45–56.

(2) Ruiz, M. L. *Alkaline nitrates and gold catalysts for Diesel soot combustion.* Doctoral thesis, Universidad Nacional de San Luis, Argentina, 2010.

(3) Ruiz, M. L.; Lick, I. D.; Ponzi, M. I.; Rodriguez-Castellón, E.; Jiménez-López, A.; Ponzi, E. N. Thermal decomposition of supported lithium nitrate catalysts. *Termochim. Acta* **2010**, *499*, 21–26.

(4) Soares, J. M.C.; Bowker, M. Low temperature CO oxidation on supported and unsupported gold compounds. *Appl. Catal., A* **2005**, *291*, 136–144.

(5) Partington, J.R. *Text-Book of Inorganic Chemistry*, Fifth ed.; McMillan and Co.: New York, 1947.

(6) Marote, P.; Durand, B.; Deloume, J. P. Reactions of Metal Salts and Alkali Metal Nitrates. Role of the Metal Precursors and Alkali Metal Ions in the Resulting Phase of Zirconia. *J. Solid State Chem.* **2002**, *163*, 202.

(7) Lick, I. D.; Carrascull, A. L.; Ponzi, M. I.; Ponzi, E. N. Zirconia-supported Cu-KNO_3 catalyst. Characterization and catalytic behavior in the catalytic combustion of soot with a NO/O_2 mixture. *Ind. Eng. Chem. Res.* **2008**, *47*, 3834–3839.

(8) Nakamoto, K. *Infrared and Raman spectra of inorganic and coordination compounds*, Wiley interscience publication; John Wiley and sons, Inc.: New York, 1997.

(9) Moulder, F.; Stickle, W. F.; Sobol, P. E.; Bomben, K. D. *Standard Spectra for Identification and Interpretation of XPS data*; Perkin Elmer, Eden Prairie, MN, 1992.

(10) Zhang, X.; Shi, H.; Xu, B.-Q.; Catal, J. Vital roles of hydroxyl groups and gold oxidation states in Au/ZrO_2 catalysts for 1,3-butadiene hydrogenation. *J. Catal.* **2011**, *279*, 75–87.

(11) Idakiev, V.; Tabakova, T.; Naydenov, A.; Yuan, Z.-Y; Su, B.-L. Gold catalysts supported on mesoporous zirconia for low-temperature water–gas shift reaction. *Appl. Catal., B* **2006**, *63*, 178–186.

(12) Huang, J.; Takei, T.; Akita, T.; Ohashi, H.; Haruta, M. Gold clusters supported on alkaline treated TS-1 for highly efficient propene epoxidation with O_2 and H_2. *Appl. Catal., B* **2010**, *95*, 430–438.

(13) Schubert, M.; Hackenberg, S.; van Veen, A.; Muhler, M.; Plzak, V.; Behm, R. CO Oxidation over Supported Gold Catalysts—"Inert" and "Active" Support Materials and Their Role for the Oxygen Supply during Reaction. *J. Catal.* **2001**, *197*, 113–122.

(14) Hadjiivanov, K. I. Identification of neutral and charged NxOx surface species by IR spectroscopy. *Catal. Rev.—Sci. Eng.* **2000**, *42*, 71–144.

1157

dx.doi.org/10.1021/ie201295s |*Ind. Eng. Chem. Res.* 2012, 51, 1150–1157